SHIELDING EFFECTIVENESS OF THE USNRDL UNDERGROUND FALLOUT SHELTER

J.F. Batter and E.T. Clarke

Report No. TO-B 62-37

20 June 1962

Contract No. N-228-(217)53803

Submitted to

U.S. Naval Radiological Defense Laboratory
San Francisco Naval Shipyard
San Francisco, California

DISCLAIMER NOTICE

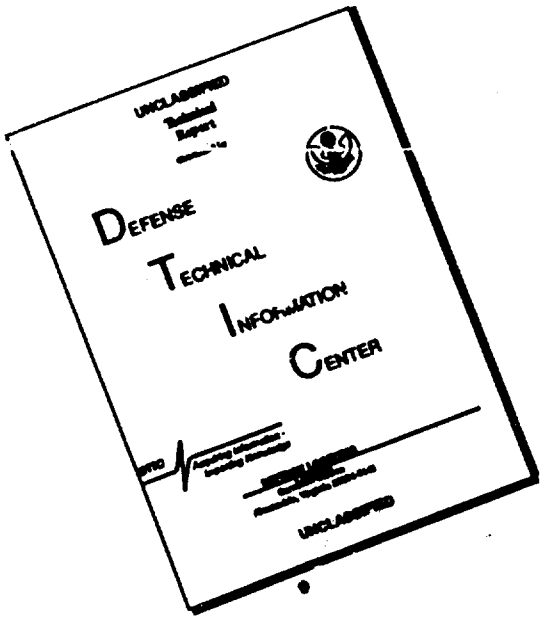

THIS DOCUMENT IS BEST QUALITY AVAILABLE. THE COPY FURNISHED TO DTIC CONTAINED A SIGNIFICANT NUMBER OF PAGES WHICH DO NOT REPRODUCE LEGIBLY.

TECHNICAL OPERATIONS incorporated

SHIELDING EFFECTIVENESS OF THE USNRDL UNDERGROUND FALLOUT SHELTER

J.F. Batter and E.T. Clarke

Report No. TO-B 62-37

20 June 1962

Contract No. N-228-(217)53803

Submitted to

U.S. Naval Radiological Defense Laboratory
San Francisco Naval Shipyard
San Francisco, California

Burlington, Massachusetts

TABLE OF CONTENTS

LIST OF ILLUSTRATIONS

LIST OF TABLES

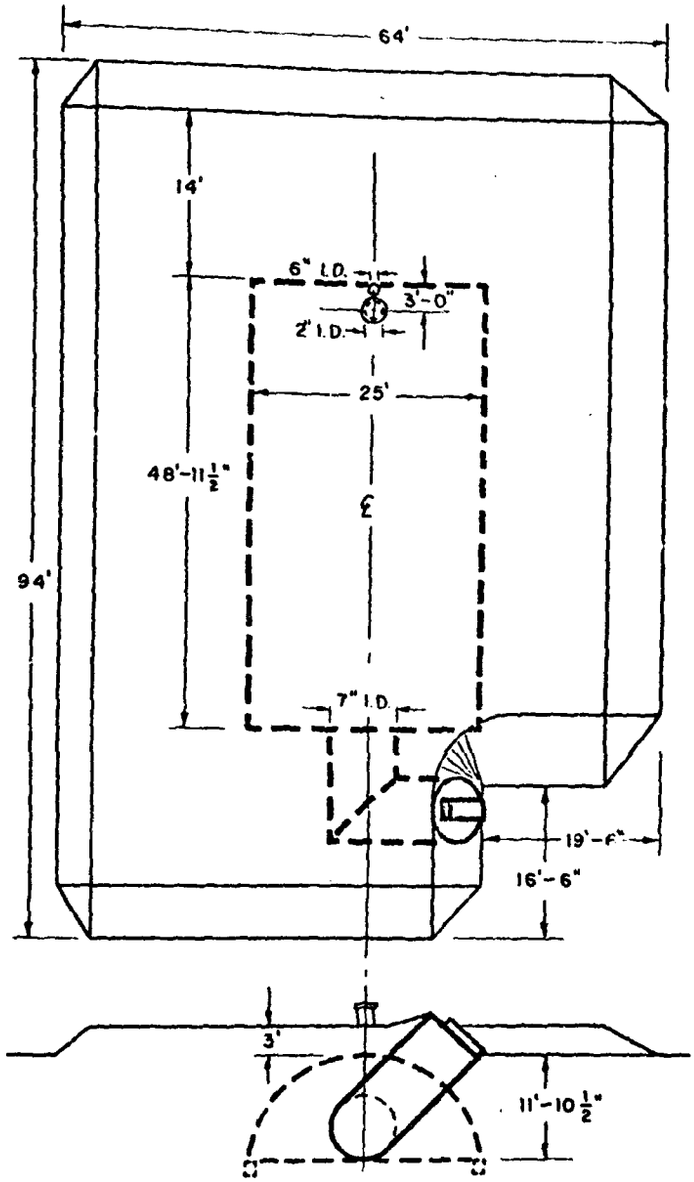

Diagram of the USNRDL Underground Fallout Shelter

CHAPTER 1

INTRODUCTION

This report presents an analysis of a series of radiation measurements of an underground ammunition magazine converted into a shelter. Data obtained by the U.S. Naval Radiological Defense Laboratory were compared with previously published theoretical and experimental work, and the protection afforded by the shelter if it were exposed to a full infinite field of contamination of either fallout or cobalt-60 was estimated. ( )

BACKGROUND

The subject of this analysis, the Naval Radiological Defense Laboratory (NRDL) shelter and the experimental measurements performed upon it, is described in the paper, "Preliminary Measurements of Shielding Effectiveness of an Underground Fallout Shelter."[1] The shelter is, in effect, a quonset hut 25 ft wide and about 49 ft long, buried so that the floor is nearly 12 ft below the ground. Earth has been packed flat over the roof so that the minimum roof cover is 2 ft 10 in. thick at the center of the hut arch.

The entrance is an L-shaped passageway that was designed to have no line-of-sight leakage path for radiation. It is of circular cross section 7 ft in diameter, and there is a 3/16-in. thick steel door covering the opening. At the rear of the shelter is a vent 2 ft in diameter with its center 3 ft from the rear wall, which is used for exhaust and for an emergency escape hatch. Radiation leakage through the entrance and the exhaust vent is of primary interest in the experiment.

Measurements of the radiation doses 46 in. above the floor were made from five simulated source areas: (1) an annulus extending from a 1 - to 5-ft radius surrounding the shelter vent, (2) an annulus extending from a 5 - to 25-ft radius also surrounding the shelter vent, (3) a 30 x 30-ft area over the roof, (4) a 25 x 50-ft area centered on the entranceway with the door covered, and (5) the same

25 x 50-ft area centered on the entranceway but with the door cleared. Area sources were simulated by circulating a 130-curie cobalt-60 source at a uniform rate through 2000 ft of polyethylene tubing laid out in suitable arrays. The radiation penetrating into the shelter was measured with time-integrating detectors.

ORGANIZATION OF THIS REPORT

The organization of this report is as follows. Chapter 2 discusses the attenuation characteristics of fallout and cobalt-60 radiation. Chapter 3 presents specific computations for extending the experimentally-measured radiation intensities to infinite-field conditions. These experimental results are compared with previously published theory. Chapter 4 presents the conclusions drawn from the study.

CHAPTER 2

COMPARISON OF FALLOUT AND COBALT-60 RADIATION

We present in this chapter some basic information on the attenuation characteristics of fallout and cobalt-60 radiation.

FALLOUT RADIATION

The energy distribution of fallout contamination, as computed by Nelms and Cooper,[2] continuously changes with time after burst. The present convention of using the 1-hr energy distribution in computing shelter factors was proposed by Spencer,[3] who reasoned that a large part of the total exposure to radiation is apt to occur during the first few hours and that calculations based on the spectrum at 1 hr after the explosion would provide a conservative estimate of the penetrability.

The energy distribution of fallout at 1.12 hr, 23.8 hr, and 9.82 days after explosion is illustrated in Figure 1. Note that, while the energy averages about 1.7 Mev at early and late times, a component at about 0.8 Mev dominates at times on the order of one day. The effect of this energy shift is illustrated in Figure 2 (reproduced from ref. 3), a plot of the relative protection provided by an underground shelter with 300 psf of earth cover vs time after nuclear explosion.

The penetration of radiation into a structure may be conveniently described by three basic geometric arrangements, as shown in Figure 3. First, there is penetration from sources adjacent to a vertical barrier (Case II); second, there is penetration from sources lying on a barrier (Case I); and third, there is penetration from sources adjacent to a horizontal barrier (Case III). The first two geometric representations may be treated in a straightforward manner, since most of the radiation penetrating the barrier comes directly from the sources rather than from scattering by the air. The third geometric representation, the penetration of radiation from sources adjacent to a horizontal barrier, also depends upon the fraction of the radiation "available" for penetration (direct radiation being "unavailable" for penetration in this case). Spencer[3] has found that an infinite plane field of fallout contamination produces approximately 9.3% of its dose as skyshine at 3 ft above the

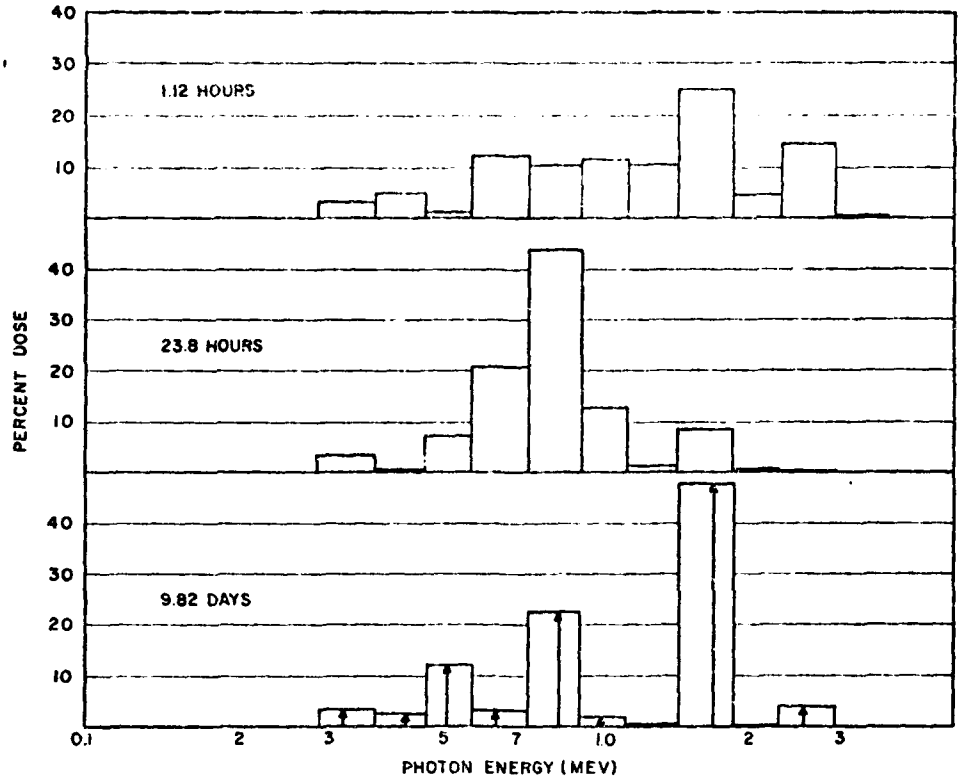

Figure 1. Distribution of Dose 3 Ft Above Infinite Plane Contaminated With Fallout of Various Ages (Volatile Products Removed)

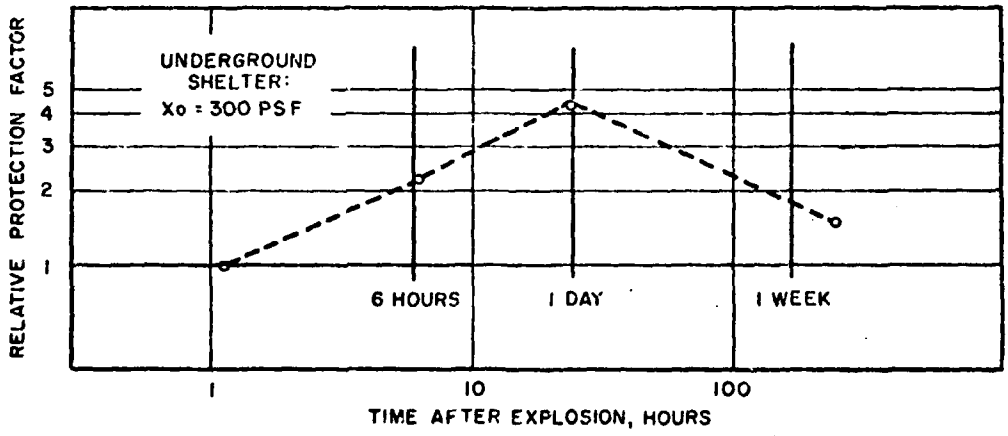

Figure 2. Variation of Protection Factor with Time

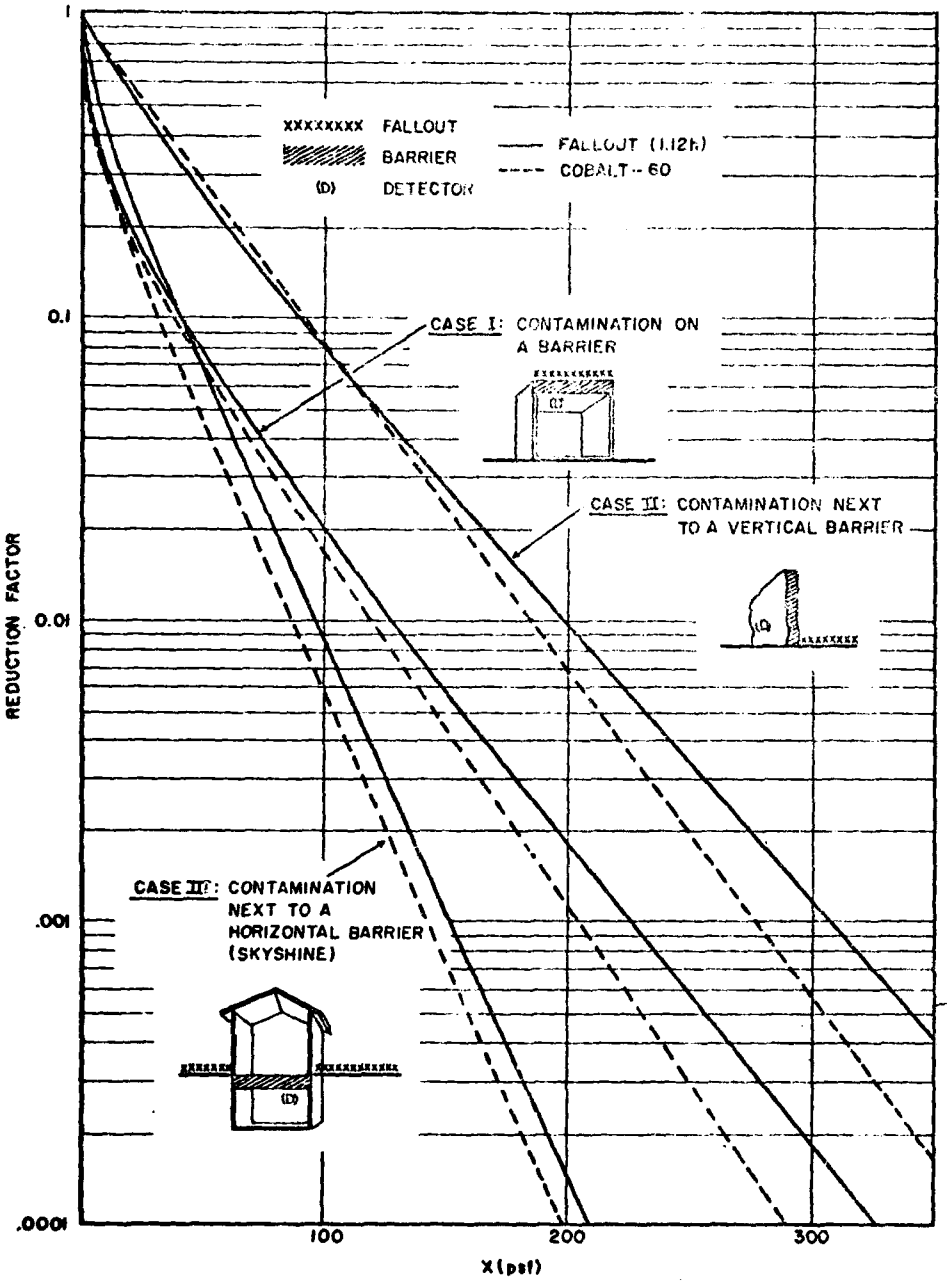

Figure 3. Penetration of 1.12-Hour Fallout and Cobalt-60 Radiation Into Concrete (from Spencer[3])

plane, while a similar field of cobalt-60 contamination produces an 8.4% skyshine component at 3-ft height. Skyshine is defined here as air-scattered radiation in the downward direction.

COBALT-60 RADIATION

The cobalt-60 skyshine fraction has been verified experimentally by Rexroad.[5] With a cobalt-60 source on the ground, Rexroad measured the dose rates at heights of 1, 3, and 6 ft above the ground for various source distances. His analysis results in buildup factors of 1.24, 1.25, and 1.28 respectively for these heights above an infinite contaminated plane. Thus, the scattered dose rate for both skyshine (radiation entering from above) and ground-scattered radiation may be computed to be 19.4%, 20%, and 21.9% of the total (direct plus scattered) radiation. The skyshine portion of the scattered intensity would be half of these values (since skyshine radiation may only penetrate from the upper 2π steradians of a sphere surrounding a detector) if the ground were assumed to be made up of air compressed to the same density as the ground.

Table 1 shows there is good agreement between Spencer's theoretical results and Rexroad's experimental results. Thus, cobalt-60, like fallout radiation, creates a skyshine field of only about 10% of the total dose rate at 3 ft above an infinite plane of contamination. Air-scattered radiation from cobalt-60 may therefore be used as a skyshine simulant if its attenuation can be related in a systematic way to the attenuation of fallout skyshine.

TABLE 1

SKYSHINE FRACTION

Height (ft)	Computed Fallout (Spencer*)	Computed Cobalt-60 (Spencer*)	Measured Cobalt-60 (Rexroad†)
1	9.8%	8.6%	9.7%
3	9.3%	8.4%	10.0%
6	8.9%	8.3%	10.9%

*See Ref. 3.

†See Ref. 5.

The attenuation to both cobalt-60 and fallout radiation afforded by a concrete barrier has been determined by Spencer[3] for the three idealized geometries, as Figure 3 shows. Because the ratio of the attenuation provided by a barrier to both fallout and cobalt radiation varies significantly with both thickness and geometry, the shelter factors measured experimentally with cobalt-60 may be corrected for fallout only in terms of these three individual geometric situations. Since the variation is regular in all cases, however, the use of an appropriate equivalent thickness computation will allow cobalt-measured protection factors to be related to fallout protection factors.

Table 2 summarizes the relative attenuation of 1.12-hr fallout and cobalt-60 radiation for various barrier thicknesses. The ratios show that results obtained by use of the cobalt-60 simulant will generally be over-optimistic. In particular, since most of the radiation reaching the underground shelter proceeds by the Case III mechanism of downward scattering, protection factors must be reduced to 2/3 of the observed (cobalt) results to yield appropriate values for 1-hr fallout radiation.

TABLE 2

RELATIVE ATTENUATION OF 1.12-HOUR FALLOUT AND COBALT-60 RADIATION

Barrier psf	Case I: Contamination on a Barrier			Case II: Contamination Next to Vertical Barrier			Case III: Contamination Next to Horizontal Barrier		
	FO	Co-60	Ratio	FO	Co-60	Ratio	FO	Co-60	Ratio
50	.078	.069	1.13	.260	.275	0.94	.067	.046	1.46
100	.020	.0165	1.21	.082	.082	1.00	.0082	.0056	1.46
150	.0057	.0042	1.34	.0275	.0235	1.16	.00106	.00071	1.49
200	.00175	.00115	1.50	.0095	.0069	1.37	.00015	------	----
250	.00055	.00029	1.90	.0034	.00205	1.66	------	------	----
300	.000185	.000076	2.45	.00122	.00056	2.18	------	------	----

CHAPTER 3

ANALYSIS

This chapter presents an estimate of the radiation dose that would have been delivered within the NRDL shelter if it had been exposed to infinite-field contamination. Considerable portions of this analysis are based directly upon the experimental data by Shumway, et al.,[1] obtained by exposing the shelter to a simulated uniformly-contaminated but limited field of cobalt radiation. No attempt has been made to analyze the shelter completely, but rather attention has been directed toward the critical areas, such as the entranceway and the vent.

SHELTER VENT AREA

The roof of the shelter contains a vent structure protruding from the shelter to a point 2.5 ft above the ground surface. This vent structure is composed of a 2-ft diameter pipe of 1/4-in. wall thickness with a 1/4-in. iron plate cover. Radiation penetration of the vent was investigated by simulating a field of contamination in two annular areas centered about the vent. These two areas, called the skyshine array and the lip array, were of 25-ft outer radius 5-ft inner radius, and 5-ft outer radius 1-ft inner radius respectively. During both exposures, the dose was measured on a 1-ft rectangular grid at a height of 46 in. above the floor. A sketch of the salient portions of the vent structure is presented in Figure 4, together with a diagram of the two areas of simulated contamination.

Since the source simulation was performed in rings, it is perhaps best to describe the calculated infinite-field dose in terms of four annular areas of radii 0 to 1 ft, 1 to 5 ft, 5 to 25 ft, and 25 to ∞ ft, and to describe the detector position in terms of its radius from the centerline of the shelter vent at a height 46 in. above the shelter floor. These doses are further differentiated according to the path by which the radiation arrives at the detector.

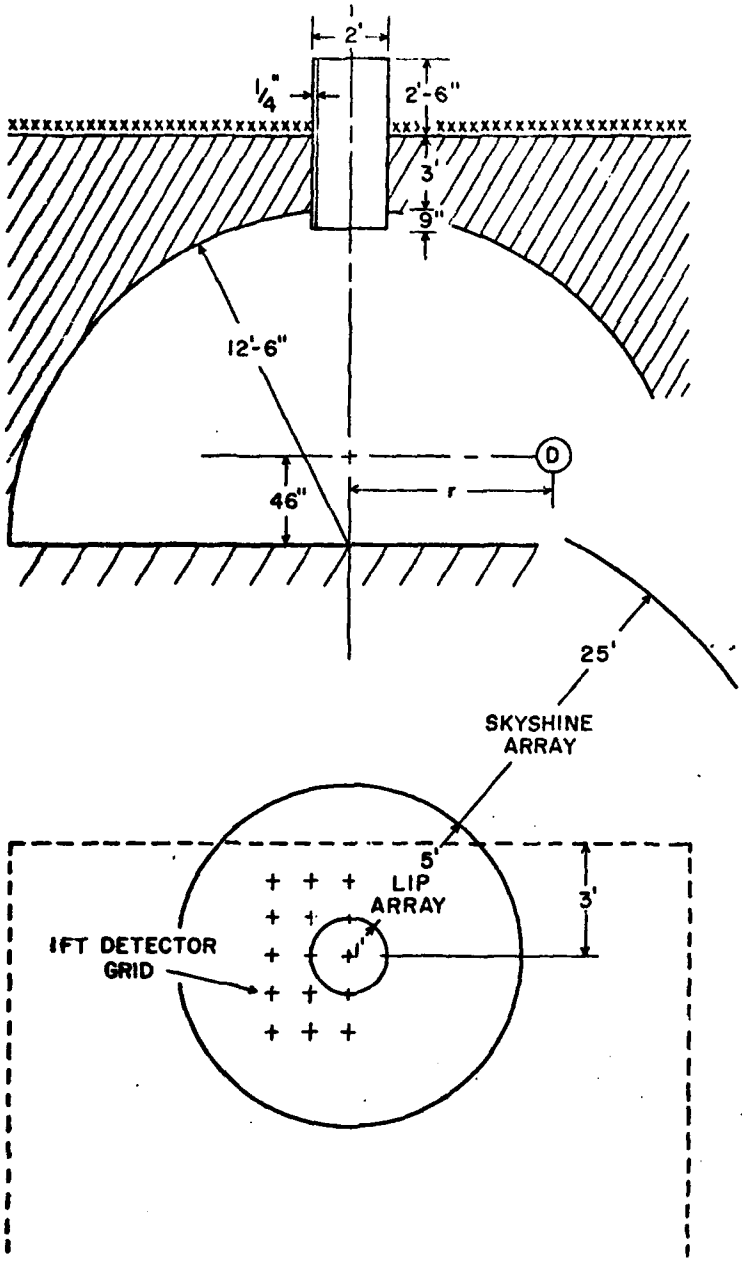

Figure 4. Vent Construction

The following components represent doses from the indicated radiation sources and scatterers to a detector located at radius, r:

D_d (0→1) = Direct radiation from sources on the vent cover

D_v (0→1) = Radiation from sources on the vent cover scattered by the walls of the vent

D_ℓ (0→1) = Radiation from sources on the vent cover scattered by the lower lip of the vent

D_f (0→1) = Radiation from sources on the vent cover scattered by the floor of the shelter

D_e (1→5) = Experimentally-measured radiation from sources in a contaminated field extending in a radius of 1 to 5 ft around the vent

D_e (5→25) = Experimentally-measured radiation from sources in a contaminated field extending in a radius of 5 to 25 ft around the vent

D_s (25→∞) = Skyshine and vent-scattered radiation from sources in a contaminated field lying beyond a 25-ft radius around the vent.

Then the total dose rate, D_t (0→∞), will be given by the sum of these seven components.

Computation of the various dose components requires data for the direct and scattered dose from each annulus and the attenuation afforded by different geometries. For purposes of clarity, the data required are summarized at this point. Table 3 presents the direct and scattered dose components for cobalt-60 radiation from the 4 annular fields at different altitudes above the field. The buildup factors used in the computation were obtained from ref. 5. The attenuations afforded by concrete (or steel) to cobalt-60 radiation for different geometrical situations are obtained from ref. 3 and are shown in Figure 3, p. 5. We shall proceed with the computation of the dose components.

THE DIRECT DOSE FROM CONTAMINATION ON THE VENT COVER, D_d (0→1)

It is difficult to compute exactly the uncollided dose reaching a detector located at radius r in the shelter from contamination existing on the vent cover, because the mass thickness between source and detector is a rapidly varying function of the

TABLE 3

DIRECT RADIATION INTENSITY (R/hr) ABOVE THE CENTER OF A CONTAMINATED AREA OF COBALT-60, 1 CURIE/FT^2

Contaminated Annulus	Ft above Plane				
	0	1	3*	6	11.67
0-1 ft	---	31	4.7 + 0.9	1.2	0.3
1-5 ft	145	115	54 + 9.8	20	6.4
5-25 ft	141	140	128 + 19	106	65
25-∞ ft	212	211	211 + 63	209	203

*Air-scattered intensities 3 ft above the plane containing the annuli are given as the second figure in this column (data based on R. E. Rexroad and M. A. Schmoke [5]). Infinite-field scattered radiation data are from L. V. Spencer.[3]

radius of the detector from the centerline of the vent. For example, a detector centered below the vent cover has essentially no mass attenuation, while a detector several feet away has an earth cover of 3 ft blocking a portion of the vent cover while it still maintains direct view of the remainder of the vent cover. Since the earth-cover thickness is large, we may approximate the uncollided dose to a detector by assuming that all photons penetrating the earth are either scattered or absorbed. Thus, the dose rate to a detector that is located away from the centerline of the vent is a function of only that area of the vent cover that may be "seen" by the detector (the source is assumed to be uniformly smeared on the vent cover) and the mean distance from the detector to the center of the visible area of the vent cover. Then, the uncollided dose reaching a detector from contamination existing on the vent cover may be calculated approximately by the relation:

$$D_d\,(0\text{-}1) \cong \frac{\pi a^2 q \sigma}{d^2} \cdot \frac{\omega(r)}{\omega(0)}\, B(x)$$

where

r = detector radius from the vent axis, ft

a = radius of source = 1 ft

q = dose conversion factor = 14.3 R/hr-curie at 1 ft

σ = source density = 1 curie/ft^2

$\omega(r)$ = solid angle fraction of the portion of vent cover seen by the detector at radius, r

d = vertical distance from the center of the source area to the detector = 14 ft

B(x) = barrier attenuation introduced by 0.25-in. thick vent cover = 0.36.

Table 4 presents the computations of the direct dose from contamination on the vent cover.

TABLE 4

THE DOSE RATE DUE TO CONTAMINATION ON COVER

	Radius, r(ft)				
	0	1	2	3	4
$\omega(r)$	.0023	.0023	.0016	.0005	0
$D_d(0\rightarrow1)$ (R/hr)	.081	.080	.056	.018	0

THE DOSE FROM SOURCES ON THE VENT COVER SCATTERED BY THE WALLS OF THE VENT, D_v (0→1)

The radiation reflected from the vent walls to a detector located at a distance r from the centerline of the vent structure may be computed by summing the components of the dose striking each differential element of wall area from each differential element of contamination area times the appropriate albedos, over all vent and wall areas. Since this task would require a computer, several simplifying assumptions were made. First, the source was assumed to be a point isotropic source of the same strength as the total cover contamination located at the center of the cover. Second, the cylindrical vent was assumed to be an octahedral vent, and the incident angle of radiation was taken as the angle between a perpendicular line to the center

of each surface area seen by the detector and a line from the center of each area through the source locations. Third, because data were lacking for the differential albedo for steel, smoothed plots of the differential albedo for concrete at 1 Mev were used.[6] Figure 5 presents the smoothed curves of this albedo for incident angles of 74.5° and 84.5°. The total dose received at a detector from radiation

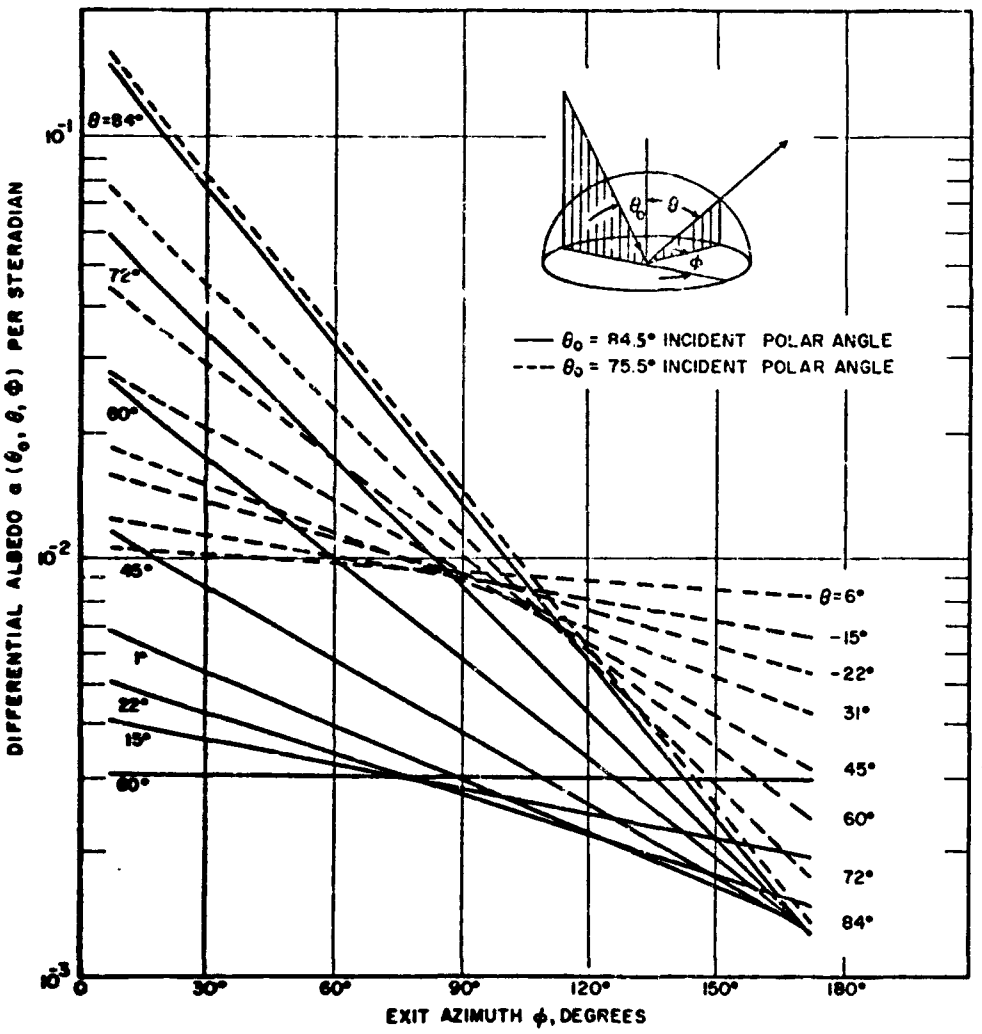

Figure 5. Smoothed Curves of the Differential Albedo Divided by the Cosine of the Incident Angle for 1-Mev Photons on Concrete

scattered from the vent wall may thus be written as follows (see Figure 6 for the angles and geometry involved):

$$D_v\,(0\rightarrow 1) = \sum_{\text{all areas}} \frac{S\,q\,A_j\,\alpha(\Theta_o,\,\Theta,\,\Phi)\cos\Theta_o\,B(x)\cos\Theta}{b^2\,c^2}$$

where

S = source strength = π curies

q = dose conversion factor = 14.3 R/hr-curie at 1 ft

A_j = area of the j^{th} wall as seen by the detector

b = distance from center of A_j to the source (ft)

c = distance from center of A_j to detector (ft)

Θ_o = polar angle of incidence of gamma ray at center of A_j area

Θ = polar angle of exit of gamma ray at center of A_j area to detector

Φ = azimuthal angle of exit of gamma ray at center of j^{th} area to detector

$\alpha(\Theta_o, \Theta, \Phi)$ = flux albedo = fraction of the dose flux impinging at polar angle, Θ_o, on area, A_j, that is reflected at azimuthal angle, Φ, and polar angle Θ, per steradian.

$B(x)$ = barrier factor for vent cover = 0.36.

Since the approximation that all radiation from the reflecting surface strikes and exits at the area's center (and hence at this same polar angle) is rather poor for dosimeters that can see the entire vent wall (radius from 0 to 1 ft), further computations were performed by dividing the area seen by the detector into 2 and 4 vertical sections and treating each section as before. Table 5 presents the dose rate contributions resulting from radiation reflected from the vent walls.

THE DOSE FROM SOURCES ON THE VENT COVER SCATTERED BY THE LOWER LIP OF THE VENT, $D_\ell\,(0\rightarrow 1)$

The dose was calculated for radiation from sources on the vent cover striking the lower lip portion of the vent and scattering to the detector located at radius r from the centerline of the vent. The procedures of LeDoux and Chilton[7] were used, which are predicated upon a rectangular-shaped duct and a point source. For

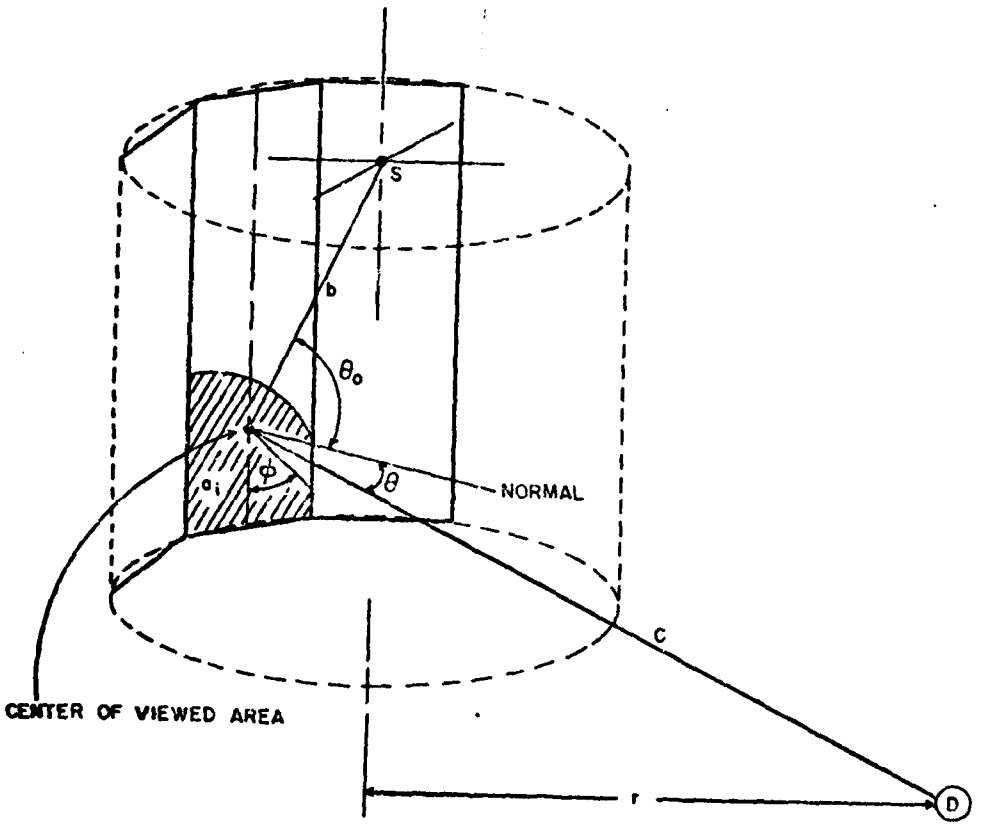

Figure 6. Idealized Vent Structure

TABLE 5

THE WALL-SCATTERED DOSE RATE (R/hr)

	Radius, r(ft)						
	0	1	2	4	6	8	10
D_v (0→1)	.0084 .0069* .0052†	.016 .012* .010†	.008	.0021	.0006	.00023	.00012

*Computed with 2 vertical area sections.

†Computed with 4 vertical area sections.

simplicity, we assumed that the cylindrical shelter vent was replaced by a rectangular vent of similar size and the area-distributed source on the vent cover was replaced by a point source of similar strength. Using LeDoux's methods, we computed the lip-scattered doses for various detector positions, which are presented in Table 6.

TABLE 6

THE LIP-SCATTERED DOSE RATE (R/hr)

	Radius, r(ft)					
	1	2	4	6	8	10
D_ℓ (0→1)	0	.034	028	.015	.0070	.0039

THE DOSE FROM RADIATION SCATTERED FROM THE FLOOR OF THE SHELTER, D_f (0→1)

The dose contribution from radiation scattered off the floor arriving at a detector located at radius r from the centerline of the vent may be approximated by summing the direct-dose rates at the floor from each differential source area on the vent cover, times the appropriate albedo, times each differential floor area, divided by the distance to the detector squared. As this procedure would require a double integration

over floor and vent cover area, the following approximation was made. The source was assumed to be a point source of total strength equal to the cover contamination, and the albedo was taken as the albedo to the center of the direct-dose illuminated floor area. The dose rate from floor-scattered radiation may thus be approximated as:

$$D_f\,(0\rightarrow 1) \cong \frac{S\,q\;\alpha(\Theta_o,\,\Theta,\,\Phi)\,A_f\cos\Theta}{g^2\,\ell^2}\;B(x),$$

where

S = source strength = π curies

q = dose conversion factor = 14.3 R/hr-curie at 1 ft

g = distance in ft from floor to vent cover

A_f = area of the floor illuminated by direct radiation

ℓ = slant distance from detector to center of illuminated floor area

$B(x)$ = attenuation of vent cover = 0.36

$\alpha(\Theta_o, \Theta, \Phi)$ = differential flux albedo per steradian.

The floor-scattered dose was computed for various detector locations and is presented in Table 7.

TABLE 7

THE FLOOR-SCATTERED RADIATION FROM SOURCES LOCATED ON THE VENT COVER (R/hr)

	Radius, r(ft)						
	0	1	2	4	6	8	10
$\alpha(\Theta_o, \Theta, \Phi)$	.010	.008	.088	.011	.014	.016	.017
$D_f\,(0\rightarrow 1)$	.0012	.0008	.0007	.00035	.00025	.00015	.00007

THE DOSE FROM TWO ANNULAR CONTAMINATED AREAS, $D_e(1\rightarrow 5)$ AND $D_e(5\rightarrow 25)$

Figures 7 and 8 show Shumway's[1] experimental data from a set of dosimeters arranged 46 in. above the floor of the shelter and at various distances from the vent axis. Figure 7 represents measurements, normalized to a contamination density of

1 curie of cobalt-60 per ft^2. obtained from an annular source of 1-ft inner radius and 5-ft outer radius. Figure 8 represents normalized dose rates for a source of 5-ft inner radius and 25-ft outer radius. In both cases. the data showed no significant variation with azimuth angle around the vent axis, indicating that most of the radiation reaching the detectors entered the shelter through the symmetrical vent. This radiation can be scattered either by the air above the vent or by the vent structure itself. We have calculated these two types of contributions to obtain their relative magnitudes and to assist in making the necessary extrapolation to infinite-contaminated-field conditions. We shall discuss these calculations for skyshine and vent-scattered radiation in the following paragraphs.

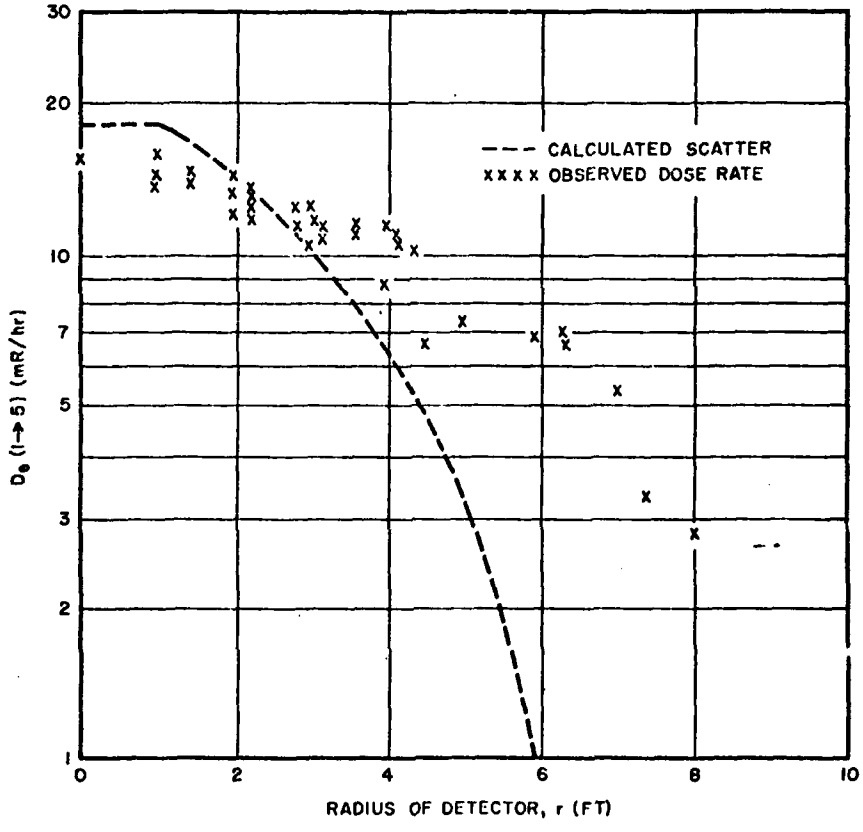

Figure 7. Observed Dose Rates Compared with Calculated Scatter from Contaminated Annuli 1- to 5-Ft Inner and Outer Radii, 46 Inches Above Floor

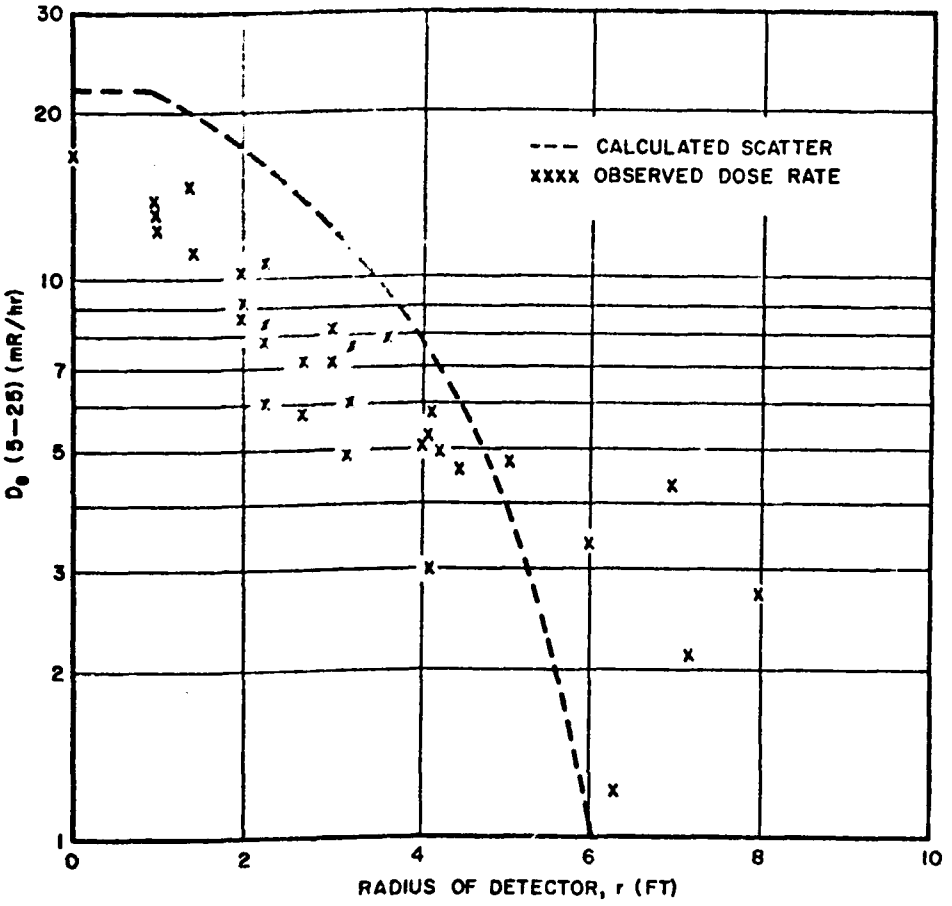

Figure 8. Observed Dose Rates Compared with Calculated Scatter from Contaminated Annuli 5- to 25-Ft Inner and Outer Radii, 46 Inches Above Floor

Skyshine

Several sources of information may be used to estimate the skyshine contribution. Schumchyk and Tiller[8] have reported that measurements of scattered doses from point sources of cobalt-60 lying on the ground at various distances from a foxhole agree reasonably well with theoretical predictions by Spencer.[3] In particular, they showed that for sources between 2 and 16 ft from the detector, the quantity $Q(\omega) = 2\pi r\, I_r(\omega)$ depends only on the solid angle fraction ω seen by the detector. Here r is the source distance from the axis of the foxhole, and I_r is the observed

dose rate in R/hr per curie. They also found that for small solid angles ($\omega < 0.2$) the variation of intensity with solid angle could be expressed as

$$\frac{I_{obs}}{S_{calc}} = \frac{\omega}{3},$$

where S_{calc} is the scattered radiation present at the top of the hole, calculated from theoretical infinite-medium buildup data. This same ratio was reported by Clarke, et al.,[9] to represent Monte Carlo calculations for predicting the scattered radiation entering an open basement surrounded by a cobalt-60 contamination field.

Now, it can be readily shown that the integrated skyshine dose rate on the axis of a hole surrounded by a contaminated annulus with radii a and b is

$$I_s(\omega) = \int_a^b (2\pi r\sigma dr)\, I_r(\omega) = \sigma \int_a^b Q(\omega)\, dr$$

$$= \sigma(b-a)\, Q(\omega)$$

since for small radii, Q was shown to be independent of r. Here σ represents the source density on the ground. Inserting data from ref. 8, the intensity on the axis is

$$I_s(\omega) = 57\, \omega\sigma(b-a)\ \text{mR/hr},$$

for $\omega < 0.2$, small radii, and σ in curies/ft^2.

For the two annuli used here, the predicted skyshine 46 in. off the floor attenuated by a factor of 0.36 by the steel vent and lid is

1-5 ft annulus: I_s = 0.31 mR/hr
5-25 ft annulus: I_s = 1.55 mR/hr.

Vent Scattering

The radiation scattered into the shelter by the vent was estimated with the aid of Monte Carlo calculations by Raso[6] giving the reflection and transmission of 1-Mev gamma radiation striking concrete. These data present the differential albedos and transmissions as functions of both polar and azimuth exit angles for several incident polar angles.

To simplify the problem, it was assumed that: (1) all incident radiation arriving at the vent travelled parallel to the ground, (2) for radiation to reach a detector in the shelter and on the cylinder axis, the exit polar angle averaged 85° and the exit azimuth was always 90°, (3) the scattered radiation was composed partly of gamma rays passing through the cylinder and emerging in the downward direction and partly of radiation passing through one side of the cylinder and scattering backward and downward from the opposite wall.

The equation used was one presented in the Addendum to ref. 6, giving the per unit incident dose rate at a point of specified distance and direction from a scatterer. The incident radiation from the contaminated annuli was considered to be almost entirely direct; its intensity is

$$D = 2\pi q\sigma \quad E_1(\mu\sqrt{h^2 + a^2}) - E_1(\mu\sqrt{h^2 + b^2}),$$

where h is the detector height, a and b are inner and outer annulus radii, μ is the air absorption coefficient = 2.24×10^{-3} per ft, and the remaining terms are those used earlier. Results of the application of this equation have been given in Table 3, p. 11.

Dose rates due to vent-scattered radiation at detectors directly beneath the vent and 46 in. above the floor were calculated to be 17 mR/hr and 21 mR/hr for the 1 to 5-ft annulus and the 5 to 25-ft annulus respectively. These rates may be compared with the observed value of 16 mR/hr found for both annuli. In addition, for radiation from the larger annulus scattering to a detector 12 ft above the shelter floor, the observed 30 mR/hr may be compared with the computed 46 mR/hr. Differences between measurements and calculations are in part attributable to the use of albedos for 1 Mev on concrete instead of the actual case of cobalt-60 (1.25 Mev) on iron and in part attributable to the assumption of a semi-infinite backscattering medium rather than the actual 1/3-mfp-thick vent wall.

Radial Distribution of Scattered Dose

The previous calculations were used to estimate the dose rate scattered to a point on the axis of the cylindrical vent. As an approximation, it was assumed that the scattered radiation from either the air or the vent was distributed isotropically

and, hence, that the dose rate would be proportional to the fraction of the vent area that could be seen by the detector. The problem is simplified to one of determining the fractional area common to two overlapping circles. These circles can be visualized by imagining the appearance of the vent when looked at from below and to one side, as illustrated in Figure 9. Then, the fractional area is:

$$\frac{2}{\pi}\left[\cos^{-1}y - y\sqrt{1-y^2}\right]$$

where $y = \frac{x}{2a} = \frac{h}{2z}\left(\frac{r}{a} - 1\right)$, permitting the intensity (as a fraction of axis value) to be calculated as a function of distance, r, from the axis.

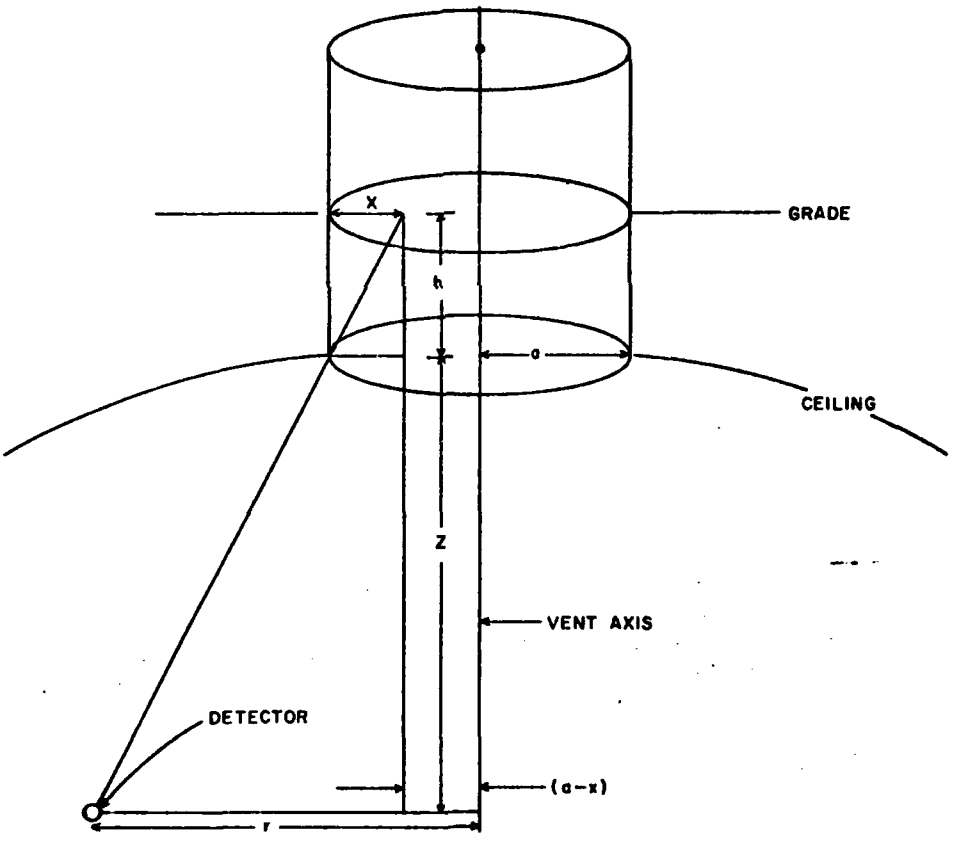

Figure 9. Geometry of the Shelter Vent

The results of these calculations are shown in Figures 7 and 8, pp. 18 and 19. There seems to be satisfactory agreement between the observed and calculated intensities, except at points at a considerable distance from the vent axis. Undoubtedly, the increased dose rates observed here are produced by further scattering from the vent walls.

THE SKYSHINE AND VENT-SCATTERED DOSE FROM THE CONTAMINATED AREA BEYOND 25 FT, D_s (25→∞)

The contribution to the shelter dose from radiation sources beyond the experimentally tested area must be calculated and added to the observed intensities. The dose rate scattered into the shelter by the vent is easy to compute; the scattered dose is proportional to the direct radiation incident on the vent. A vent-scattered dose rate of 32 mR/hr from the far-field beyond 25 ft is thus obtained from the scattered-dose rates due to the annuli.

Skyshine is obtained in a different way. Table 3 (p. 11) gives the total skyshine for a contaminated field beyond 25 ft as 63 R/hr; this was obtained by subtracting the annular rates from the theoretical scatter due to an infinite field (ref. 3, Figs. 28.3 and B-15). In penetrating to the detector in the shelter, this skyshine is attenuated (0.36) by the thickness of the steel vent and by the solid-angle fraction (0.004) subtended by the vent opening. This solid-angle fraction produces a geometrical attenuation of 0.001 shown as an extrapolation of Figure B.37 of ref. 3. The net result is a calculated skyshine of 23 mR/hr due to contamination beyond 25 ft.

The combined dose rate of 55 mR/hr represents the expected intensity on the vent axis 46 in. above the floor. As an approximation, it is expected that the distribution of intensity with radius from the axis should follow the same pattern as that for the annuli.

TOTAL DOSE RATE, D_t (0→∞)

The total dose rate in the shelter due to the radiation from an infinite field of cobalt-60 (1 curie/ft^2) penetrating the shelter vent can now be estimated by summing the various contributions. These are summarized in Table 8.

TABLE 8

DOSE RATES (mR/hr) 46 IN. ABOVE THE SHELTER FLOOR DUE TO 1 CURIE/FT^2 COBALT-60 ON SURFACE*

	Radius, r(ft)						
	0	1	2	4	6	8	10
D_d (0→1)	81	80	56	0	0	0	0
D_v (0→1)	5	10	8	2	0.6	0.2	0.1
D_ℓ (0→1)	0	0	34	28	15	7	4
D_f (0→1)	1.2	0.8	0.7	0.35	0.25	0.15	0.07
D_e (1→5)†	15.4	14.5	13	9.5	5.8	2.8	1.0
D_e (5→25)†	17	13	10	5.8	3.4	2.0	1.1
D_s (25→∞)	55	55	43	20	2.5	0	0
D_t (0→∞)	175	173	165	66	27	12	6

*Surface dose rate is 500 R/hr at 3 ft.

†D_e values are means of experimental data.

SHELTER ENTRANCEWAY

The NRDL underground shelter entranceway is an L-shaped passage designed to have no line-of-sight leakage path for radiation. The entranceway is composed of a 7-ft-diameter tube inclined at a 45° angle to the earth's surface, penetrating to a depth of approximately 12 ft where it is connected to a 7-ft-diameter tube running horizontally for approximately 12 ft to the shelter. The outer portal of the entranceway is covered with a 3/16-in.-thick cover plate. Figure 10 illustrates the pertinent features of the entranceway.

Shumway[1] of NRDL exposed the entranceway to a rectangular contaminated field of cobalt-60. Two experiments were performed with this source array. In the first experiment, contamination was simulated over the entire area including the entranceway cover. The second experiment was a duplicate of the first, except that the entranceway cover was left uncontaminated. This pair of experiments provides an opportunity to test the methods for computing radiation penetration of right-angle

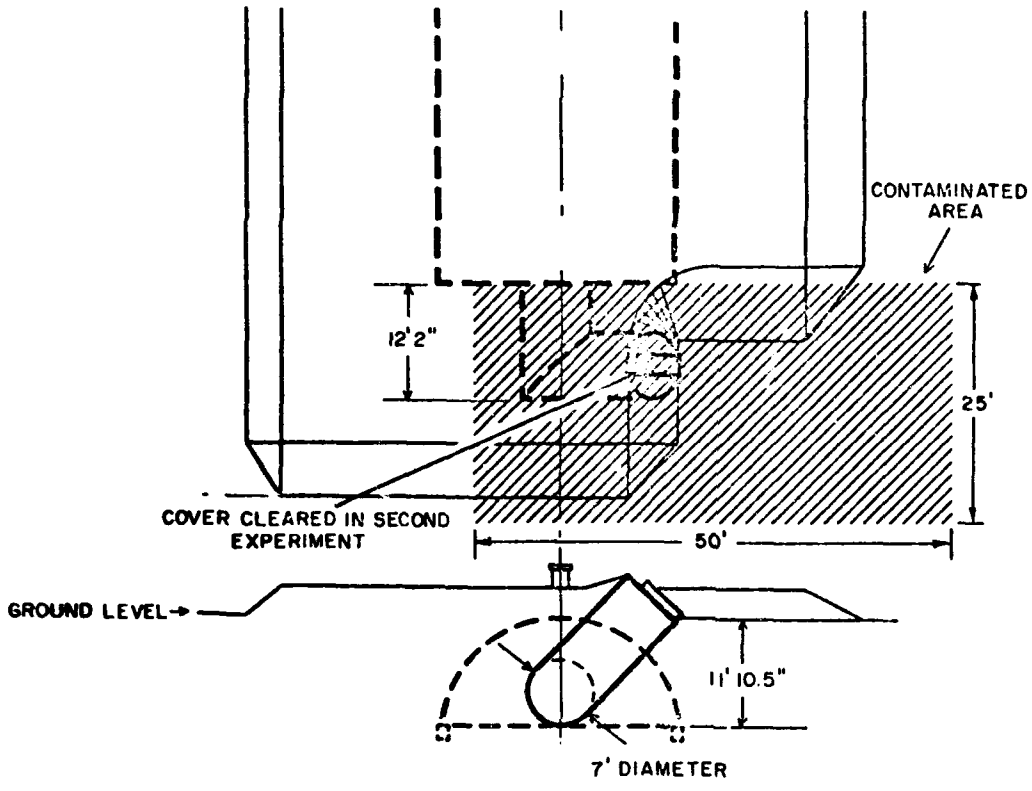

Figure 10. The Shelter Entranceway

ducts suggested by LeDoux, et al.,[7] and Eisenhauer.[12] Shumway's observations along the centerline of the horizontal tube are presented in Table 9 as a function of distance from the junction of the centerlines of the two legs of the duct. The differences should be attributable to contamination on the entranceway cover.

Eisenhauer, in his technical note on the scattering of radiation in ducts,[12] presents experimentally-measured data on 3 ducts of rectangular cross section containing a right-angle bend. He shows from single-scatter theory that the dose in the second leg should be expressible by the equation

$$D/D_o = .090\omega$$

where

D = dose rate along the centerline of the horizontal leg

D_o = dose rate at the junction of the centerlines of the first and second leg

ω = the solid-angle fraction subtended at the detector by the junction.

When the solid angle was defined in terms of the duct cross section and the detector distance from the near side of the intersection, his experimentally-obtained data were found to agree with this equation for distances of several diameters from the junction.

TABLE 9

OBSERVED DOSE RATES IN THE HORIZONTAL ENTRANCEWAY DUE TO AREAS CONTAMINATED WITH 1 CURIE/FT^2 COBALT-60*

Distance from Centerline Junction (ft)	Entry Cover Contaminated (R/hr)	Entry Cover Clear (R/hr)	Difference (R/hr)
0	2.60	0.480	2.12
2.8	2.70	0.510	2.19
3.5	1.90	0.460	1.44
5.5	0.330	0.114	0.216
7.5	0.044	0.025	0.019
9	0.022	0.0073	0.0147
12	0.0091	0.0023	0.0068
15	0.0053	0.0019	0.0034

*Surface dose rate is 500 R/hr at 3 ft.

A second approach to the problem is presented by LeDoux,[7] who divides the junction of the two ducts into several suitable areas and computes the dose contribution of each area by a straightforward albedo approach. Correction terms are applied to account for the corner "lip effect." Because differential albedo data were not available at the time, LeDoux used the results of Monte Carlo calculations

by Berger and Raso,[10] who reported albedos of surfaces irradiated at various incident polar angles. LeDoux assumed that the backscattered currents were distributed isotropically and calculated differential albedos accordingly. The agreement with Eisenhauer's experimental data was good. Raso,[6] however, has since calculated differential dose albedos of 1-Mev photons incident on concrete, and we therefore attempted to modify LeDoux's work with this more recent information. A plot of Raso's data on differential dose albedos applicable to this calculation is shown in Figure 11, along with curves representing LeDoux's assumed values. The particular directions were chosen because they cover the four scattering surfaces at the elbow of a square duct.

For computational purposes, the cylindrical entranceway of the NRDL shelter was replaced by a square entranceway of equal cross-sectional area, since both methods described above were based on rectangular ducts. The results of these calculations are shown in Table 10 in terms of the ratio of observed-to-calculated reductions in intensity relative to the radiation intensity incident on the junction midpoint. (The measured intensity of the radiation incident on the junction agreed closely with the value calculated for the contaminated entry cover.)

TABLE 10

COMPARISON BETWEEN CALCULATED AND OBSERVED INTENSITIES ALONG THE HORIZONTAL ENTRANCEWAY

Distance from Junction (ft)	Observed/Calculated Intensity		
	Eisenhauer	LeDoux Isotropic Albedos	LeDoux, Raso Albedos
7.5	0.36	0.32	0.52
9	0.44	0.36	0.65
12	0.44	0.41	0.80
15	0.40	0.36	0.70

All three computations produced larger scattered-dose rates than were actually observed. The agreement between Eisenhauer's and LeDoux's isotropic-computed dose rates was to be expected, since both had been checked against Eisenhauer's

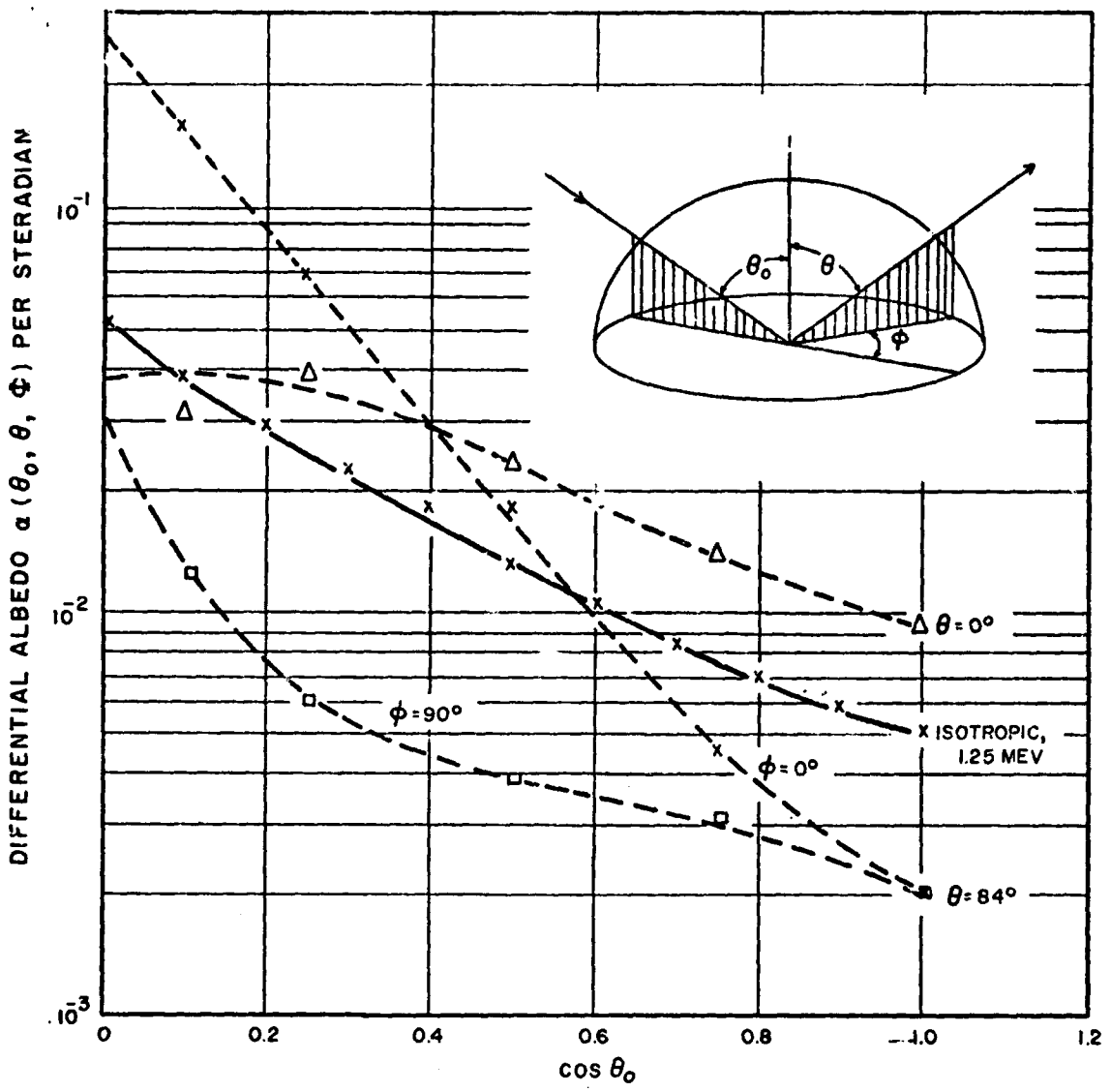

Figure 11. Differential Dose Albedos of 1 Mev on Concrete, from Several Particular Directions

experimental data. The difference between the two LeDoux calculations is due to differences in the assumed albedos, which in part may be ascribed to the use of 1 Mev rather than 1.25 Mev Monte Carlo data. But there is clearly a factor of from 2 to 3 between the NRDL shelter measurements and those originally made on the concrete ducts.

The extra shielding demonstrated by the NRDL design may result from the corrugated shape of the tube comprising the entranceway. The effect of these corrugations would be to make the incident angle of the primary radiation more nearly normal, thereby reducing the albedo from the higher values characteristic of grazing radiation. The fact that part of the surface is shielded by these corrugations does not affect the albedo, since the total flux striking the surface is not changed by surface roughness.

It is also of interest to estimate the effect of far-field skyshine radiation penetrating the shelter entranceway. An approximate method of estimating the effects of far-field skyshine radiation has been previously discussed (p. 23). Skyshine radiation down a hole was shown to follow the relationship,

$$I/I_o = \frac{B(x)\,\omega}{3} \text{ for } \omega < 0.3,$$

where

I = the skyshine-dose rate

I_o = the scattered-dose rate at the entrance to the hole

ω = solid-angle fraction of the mouth of the hole from the detector

$B(x)$ = barrier factor introduced by the hole cover = 0.43 for a 3/16-in.-thick iron cover.

The quantity, I_o, may be approximated by assuming that the 25 x 50-ft rectangular source area is replaced by an annular area of the same size, centered on the entranceway, and calculating the scattered-dose rate to be expected from sources lying beyond that area. Using the buildup factors measured by Rexroad,[5] with the source at ground level and the detector at 1 ft height as before, I_o is found to be equal to 68.3 R/hr.

Table 11 presents the calculated values of far-field skyshine together with the experimentally-measured values of dose contribution from a 25 x 50-ft rectangular source area with the entranceway cover cleared, the dose contribution from a contaminated entranceway cover, and the total of all contributions.

TABLE 11

TOTAL DOSE RATE (R/hr) IN THE SHELTER ENTRANCEWAY FOR A UNIFORMLY-CONTAMINATED INFINITE FIELD OF 1 CURIE/FT^2 COBALT-60*

	Centerline Distance From Entranceway Cover, Ft			
	7	10	13	16.25
Far-Field Skyshine	1.1	0.6	0.37	0.24
Inner Rectangular Area	4.9	2.0	0.95	0.48
Entranceway Cover	13.1	5.2	3.25	2.12
Total Dose	19.1	7.8	4.57	2.84

*Surface dose rate is 500 R/hr at 3 ft.

GROUND PENETRATION

The NRDL underground shelter resembles a quonset hut approximately 49 ft long, with an arch of approximately 12.5-ft radius. A clay-like substance with a density of 1.68 when compacted, 1.37 when uncompacted, and 1.46 when wet was used to cover the shelter. The minimum earth cover at the center of the arch varied from 3 ft 8 in. near the entranceway of the quonset hut to 2 ft 10 in. near the rear of the structure. The earth was allowed to settle naturally and desiccate. For computational purposes, a density of 1.46 will be used.

Experimental measurements of the attenuation afforded by this earth cover against cobalt-60 radiation were performed and reported by Shumway.[1] The experiment consisted of centering a simulated, uniformly-contaminated 30 x 30-ft field over the shelter with one edge in the plane of the shelter's front wall (entranceway wall), as shown in Figure 12.

Because a portion of the array could shine into the entranceway, only data due to sources kept removed from the entranceway were used for comparison of computational and experimental results. Dose rates of 1 to 2 mR/hr with an uncertainty of ±0.4 mR/hr were measured from a field of 1 curie/ft^2 source density. The depth

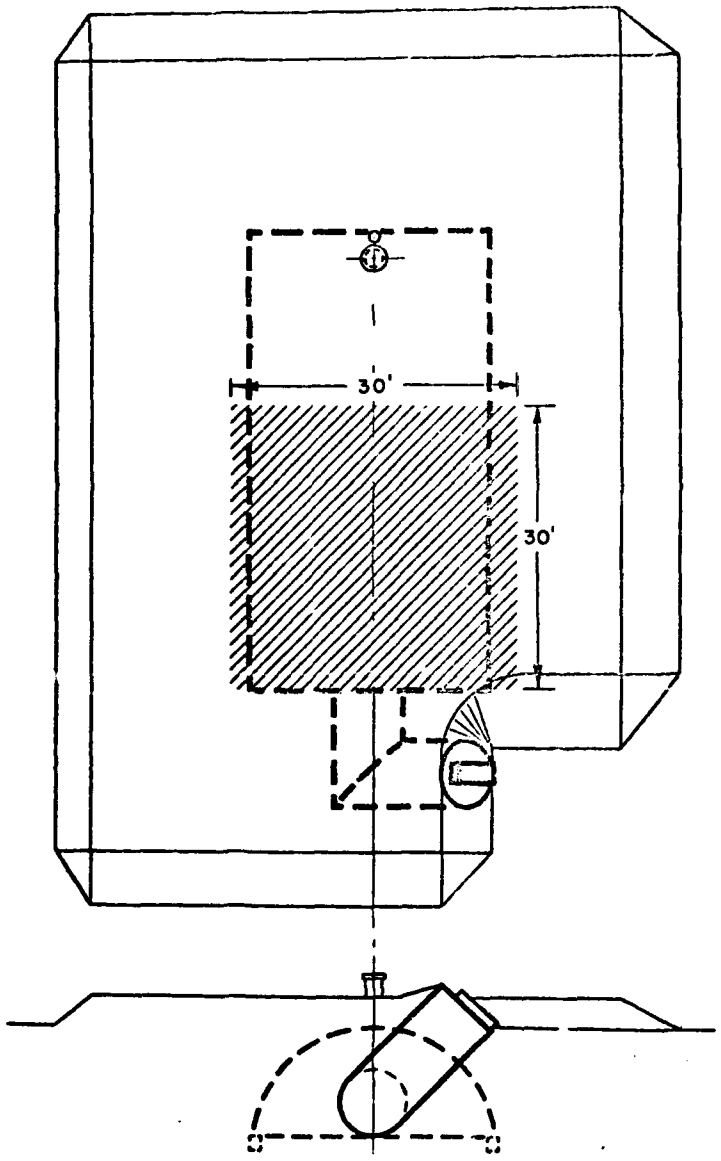

Figure 12. Contaminated Field Distribution on the Shelter Roof

of earth cover varied over the experimental area from a maximum of 3 ft 8 in. to a minimum of 3 ft 5 in. over the center of the arch. Thus, for computational purposes, an average value of 3 ft 6 in. will be used. This value, together with the best estimate of earth density ($\rho = 1.46$), provides an estimated average value of earth cover of 320 lbs/ft^2 at the arch center.

Three methods of computing the attenuation of an arch-type shelter are available in the published literature. One method is by LeDoux[13] of the U.S. Naval Civil Engineering Laboratory. LeDoux proposes that the attenuation afforded by an underground shelter is equivalent to the attenuation of an earthen slab of thickness equal to the shelter minimum roof thickness times a geometry factor. The geometry factor is based on an analysis of radiation penetrating the shelter from discrete sources lying on the ground above, using an exponential approximation for the build-up factor. For a horizontal semicircular cylindrical shelter, his results lead to a geometry factor of

$$\frac{1}{6}\left(1 + \frac{10}{2 + h/t}\right),$$

where h is the radius of the shelter arch, and t is the minimum earth-cover distance. This factor, effectively independent of energy, applies to the intensity on the floor of the shelter.

Malich and Beach[15] state that the dose rates at the centerline of an arched shelter 3 ft above the floor are well represented by 90% of the dose rate that would be received in a shelter with a slab roof of thickness equal to the minimum earth cover of an arched shelter. Malich and Beach attribute this to the fact that over 90% of the dose rate within a shelter comes from a relatively small circle on the ground directly above the detector. The radius of this circle ranges from 2.6 ft at a depth of 3 ft to 4.8 ft at a depth of 10 ft. Thus, we may assume that the experimental 30 x 30-ft source area adequately represented an infinite field for ground penetration measurements.

A third method by Spencer[3] provides detailed information for both cobalt-60 and 1.12-hr fallout radiation on the angular distribution of the radiation dose penetrating various thicknesses of earth, thus allowing the summation of radiation components from each individual increment of source area. Since the NRDL shelter

was symmetric about the vertical plane extending from the floor through the shelter arch, differential strips of 1-ft wide contamination extending the length of the shelter were used in computing the dose rate on the centerline 3 ft above the shelter floor.

Spencer (ref. 3, Fig. B-13) also provides information on the attenuation provided by a slab covered with cobalt-60: for 320 psf, the reduction factor relative to the dose rate at 3 ft above the contaminated plane is 4.5×10^{-5}. This will reduce an external field of 500 R/hr at 3 ft to about 22 mR/hr. Table 12 compares the dose rates for the cylindrical shelter calculated using these three methods with the dose rates obtained experimentally.

TABLE 12

GROUND PENETRATION OF COBALT-60 RADIATION FOR 500 R/hr EXTERNAL FIELD (1 CURIE/FT^2)

	Experimental (Shumway)	Calculated		
		LeDoux	Malich & Beach	Spencer
Geometry Factor	---	0.47	0.90	---
mR/hr in Shelter	2	10	20	16
Reduction Factor	4×10^{-6}	2×10^{-5}	4×10^{-5}	3×10^{-5}

The agreement between experiment and computation is poor. Even if we assume that the soil density is the maximum compacted value producing a minimum overhead mass of 370 psf, attenuation is increased by only a factor of 3. To try to resolve the disagreement, we analyzed data obtained by Strope[11] on a buried quonset-type shelter similar to the NRDL shelter, which was subjected to actual fallout from a nuclear weapon test. The results of these computations, shown in Table 13, are in fair agreement with the experimental data. Thus, the discrepancy between computed and measured attenuation for the NRDL shelter may probably be attributed to an error in the measurement of earth-cover thickness or density.

It is to be noted that the reduction factors for ground penetration of fallout radiation are appreciably greater than those for penetration of cobalt-60 radiation and that, under attack conditions, the radiation penetrating the interior of the

shelter through the roof may not be negligible compared to that coming through the vent and the entranceway.

TABLE 13

GROUND PENETRATION OF FALLOUT RADIATION FOR 2.2 R/hr EXTERNAL FIELD

	Experimental (ITR-1464)	Calculated		
		LeDoux	Malich & Beach	Spencer
Geometry Factor	----	0.47	0.90	----
mR/h in Shelter	0.22	0.12	0.22	0.25
Reduction Factor	1×10^{-4}	5×10^{-5}	1×10^{-4}	1.2×10^{-4}

CHAPTER 4

CONCLUSIONS

Table 14 summarizes the estimates of radiation levels expected to prevail in the underground shelter if the ground above were covered with an infinite plane of cobalt-60 of density 1 curie/ft^2, corresponding to 500 R/hr measured 3 ft above the plane.

TABLE 14

INTERIOR DOSE RATES DUE TO COBALT-60 AND FALLOUT FIELDS OF 500 R/hr AT 3 FT ABOVE SURFACE

Mode of Penetration	Point of Measurement (3 ft above floor)	Intensity (mR/hr)	
		Cobalt-60	Fallout
Through roof	Throughout shelter	2	65
Through vent	Directly below vent	175	225
	6 ft away	27	40
	10 ft away	6	9
Through entranceway (lid contaminated)	At lower door into shelter	22	33
	6 ft into shelter	5	8
Through entranceway (lid cleared)	At lower door into shelter	7	10
	6 ft into shelter	2	3

By applying the appropriate factors from Table 2 (p. 7), we can arrive at the expected intensities to be found in the shelter when equal intensity fallout radiation (500 R/hr 3 ft above the surface) is generated by close-in fallout 1 hr old.

It may be concluded that over most of its floor area the shelter offers protection factors of 100, 000 against fallout radiation and factors greater than 10, 000 everywhere except within 6 ft of the vent centerline. The two weak areas are under the vent and near the entranceway. If contamination can be cleared from the lid of the entranceway, the levels near the door can be halved.

REFERENCES

1. B.W. Shumway, et al., "Preliminary Measurements of Shielding Effectiveness of an Underground Fallout Shelter," U.S. Naval Radiological Defense Laboratory, Report R & L No. 110 (NRDL-OCDM Shielding Symposium Proceedings, October 31 — November 1, 1960).

2. A.T. Nelms and J.W. Cooper, Health Physics 1, 427-441 (1958).

3. L.V. Spencer, "Structure Shielding Against Fallout Radiation from Nuclear Weapons," Office of Civil Defense, Washington, D.C. (March, 1961).

4. M.J. Berger and J.C. Lamkin, J. Research Natl. Bur. Standards 60, 2 109-116 (1958).

5. R.E. Rexroad and M.A. Schmoke, "Scattered Radiation and Far-Field Dose Rates from Distributed Cobalt-60 and Cesium-137 Sources," Nuclear Defense Laboratory, U.S. Army Chemical Corps, Report No. NDL-TR-2 (September, 1960).

6. D.J. Raso, "Monte Carlo Calculations on the Reflection and Transmission of Scattered Gamma Radiations," Technical Operations, Inc., Report No. TO-B 61-39 (July, 1961).

7. J.C. LeDoux and A.B. Chilton, "Attenuation of Gamma Radiation Through Two-Legged Rectangular Ducts and Shelter Entranceways—An Analytical Approach," U.S. Naval Civil Engineering Laboratory, Report No. USNCEL-TN-383 (20 January 1961).

8. M.J. Schumchyk and H.J. Tiller, "Ground-Penetrating Radiation in a Foxhole from a Fallout Field of Simulated Cobalt-60," Nuclear Defense Laboratory, U.S. Army Chemical Corps, Report No. NDL-TR-3 (3 December 1960).

9. E.T. Clarke, J.F. Batter, and A.L. Kaplan, "Measurement of Attenuation in Existing Structures of Radiation from Simulated Fallout," Technical Operations, Inc., Report No. TO-B 59-4 (27 April 1959).

10. M.J. Berger and D.J. Raso, "Backscattering of Gamma Rays," National Bureau of Standards, Report No. NBS-5982 (July, 1958).

11. W.E. Strope, "Evaluation of Countermeasure System Components and Operational Procedures," Atomic Energy Commission, Plumbbob Project 32.3, Report No. ITR-1464 (14 February 1958).

12. C. Eisenhauer, "Scattering of Cobalt-60 Gamma Radiation in Air Ducts," National Bureau of Standards, Report No. NBS-TN-74 (October, 1960).

13. J.C. LeDoux, "Nuclear Radiation Shielding Provided by Buried Shelters," U.S. Naval Civil Engineering Laboratory, Report No. USNCEL-TR-025 (27 October 1959).

14. J.C. LeDoux and L.K. Donovan, "Shielding Factors for Underground Shelters of Various Geometric Shapes," U.S. Naval Civil Engineering Laboratory, Report No. USNCEL-TR-080 (5 April 1961).

15. C.W. Malich and L.A. Beach, "Radiation Protection Afforded by Barracks and Underground Shelters," Naval Research Laboratory, Report No. NRL-5017 (18 September 1957).